

On The Distribution of Bayesian Evidences

Ryan E. Keeley*

*Department of Physics, University of California Merced,
5200 North Lake Road, Merced, CA 95343, USA and
Korea Astronomy and Space Science Institute (KASI),
776 Daedeok-daero, Yuseong-gu, Daejeon 34055, Korea*

Arman Shafieloo†

*Korea Astronomy and Space Science Institute (KASI),
776 Daedeok-daero, Yuseong-gu, Daejeon 34055, Korea and
KASI Campus, University of Science and Technology,
217 Gajeong-ro, Yuseong-gu, Daejeon 34113, Korea*

(Dated: November 9, 2021)

We look at the distribution of the Bayesian evidence for mock realizations of supernova and baryon acoustic oscillation data. The ratios of Bayesian evidences of different models are often used to perform model selection. The significance of these Bayes factors are then interpreted using scales such as the Jeffreys or Kass & Raftery scale. First, we demonstrate how to use the evidence itself to validate the model, that is to say how well a model fits the data, regardless of how well other models perform. The basic idea is that if, for some real dataset a model's evidence lies outside the distribution of evidences that result when the same fiducial model that generates the datasets is used for the analysis, then the model in question is robustly ruled out. Further, we show how to asses the significance of a hypothetically computed Bayes factor. We show that range of the distribution of Bayes factors can greatly depend on the models in question and also the number of independent degrees of freedom in the dataset. Thus, we have demonstrated that the significance of Bayes factors need to be calculated for each unique dataset.

I. INTRODUCTION

Modern cosmology, in its current “precision era”, requires a thorough understanding of the employed statistical methodology in order to make robust inferences from the data. This is especially important with regards to understanding the plethora of statistical “tensions” that have cropped up in the past years, which have the potential to challenge the current concordance model of cosmology Λ CDM (cosmological constant dark energy; cold dark matter). The most notorious tension is the “ H_0 tension” which is the disagreement between the local expansion rate inferred by Planck’s measurement of the cosmic microwave background (CMB) [24] and that value directly measured by observations of Cepheids by the SH0ES collaboration [27]. These tensions are often investigated in terms of a model selection question where the Λ CDM model is compared to some new model. The comparison is typically performed by computing the Bayes factor $B_{ij} = \log Z_i/Z_j$ where Z is evidence, $P(D|M_{i,j})$, the probability of the data, D , given model $M_{i,j}$. If $B_{ij} > 0$ the model i is favored over model j and vice versa.

There are a few drawbacks to this inference procedure. The first problem is that this procedure is inherently a comparison; it can only determine which model is better or worse, not whether either model is a good fit to the

data in an absolute sense. This is an important point to keep in mind since there is no reason to believe that the true model of the Universe, whatever it may be, could be guessed at and so included as a discrete choice in this model selection procedure.

The second drawback is a question of significance. The mathematics of the procedure returns a number. It is a further step of human interpretation to decide what that number means in terms of whether we should believe one model is true and the other is false. This interpretation is commonly done with one of the two commonly used scales, the Jeffreys scale [11] and the Kass & Raftery scale [12]. However, these scales are not a one size fits all solution. Of course, determining a criteria for mapping the value of a statistic and significance is arbitrary and so either of these scales could serve as the mapping between the statistic and significance. However, physics already employs a criteria to determine whether a signal is significant, the oft-quoted “5 σ ” p -value. A p -value is the probability of observing a signal given that a null hypothesis is true. This p -value is a frequentist statistic so, at first, it may seem counter intuitive to use a frequentist criteria for a Bayesian calculation. However, it is a meaningful question to ask what is the distribution of any statistic over different realizations of the data, even the Bayesian evidence.

A third drawback is that Bayesian evidences generally depend on the subjective choice of a prior. Common choices of such a prior includes the flat prior, where the prior probability of a value of a parameter being true is uniform over some domain. This is often a good choice since such a flat prior reflects a maximum amount of ag-

* rkeeley@ucmerced.edu

† shafieloo@kasi.re.kr

nosticism about the value of a parameter. However, flat priors are not invariant under changes in parameterization. e.g. flat in $P(\theta)$ is not flat in $P(\log \theta)$. Further, any uniform distribution is only well-defined if the domain is finite e.g. we might say Ω_m is free to vary in the range $[0, 1]$. However, since the Bayesian evidence is the average of the likelihood over the prior volume, if the volume were expanded to include regions of low likelihood, then the evidence will decrease.

Previous studies have investigated the utility of Bayes factors and the Jeffreys scale for performing model selection. For instance, Nesseris & García-Bellido [22] calculate false positive and false negative rates when using the Jeffreys scale to select a particular class of models. Specifically, the models they consider have predictions that are linear in their parameters. The different models considered in that paper are all nested with different numbers of parameters. That is, model M_2 has one extra parameter compared to M_1 and for a certain value for that extra parameter, reduces to M_1 . The authors show that the Jeffreys scale can fail to penalize extra degrees of freedom when mock data was generated from the simpler model. They show that the frequency of this failure is influenced by the choice of prior. The authors conclude that the Bayes factor should not be the only tool used for model selection.

Another recent, companion paper points out related short comings of using the Bayes factor. Specifically, Koo et al. [16] demonstrate that, if the true model is not an option when calculating Bayes factors, such a scheme will still pick some false model as being best and thus not rule it out. They go on to show that the distribution of likelihoods from the iterative smoothing method can rule out all false models [17]. The current work takes inspiration from these likelihood distributions from the smoothing method and shows how to use a models' evidence alone, not the Bayes factors, to determine if a model is a good fit to the data regardless of how well other models perform.

In this paper, we seek to develop a methodology to address these two drawbacks of Bayesian calculations. We first calculate the distribution of the Bayesian evidence, for datasets commonly used in cosmology, and show how to use this distribution to answer the question of whether a model is a good fit to the data, irrespective of other models. Further, for these same datasets, we show what Bayes factors correspond to the frequentist p -value formulation of significance.

II. MOCK DATA

The approach to calculating the distribution of the Bayesian evidence is to generate a hundred mock realizations of the data and then calculate the Bayesian evidence for each one. The datasets that we use for this calculation are mock future supernova (SN) datasets as might be expected from the WFIRST telescope [8, 30] and future baryon acoustic oscillation (BAO) datasets as

might be expected from DESI [6, 7]

Type Ia SN are one of the observational pillars that built the Λ CDM model and directly measure the acceleration of the Universe. Existing SN datasets have all shown broad consistency with the Λ CDM model despite concerted searches for new physics or systematics [2, 3, 9, 14, 15, 18, 19, 23, 25, 26, 29, 31]. These successes of SN exist because they are standardizable candles; the measurement and fitting of the light-curve of the SN allows us to infer the luminosity of the SN (up to a global calibration) [2, 3, 9, 18, 23, 25, 26, 29, 31], and thus measuring the flux is equivalent to measuring a luminosity distance, or equivalently a distance moduli:

$$\mu(z) = 5 \log_{10} D_L(z) + 25 = m_B(z) - M_B + \alpha x - \beta C. \quad (1)$$

Here, μ is the distance modulus, D_L is the luminosity distance, m_B is the peak B-band flux, M_B is the absolute magnitude of SN and serves as the parameter that calibrates the distance redshift relation, and α and β are hyperparameters that control how the light-curve parameters (X_1 and C) influence the distance-redshift relation. In our mock dataset, we imagine the case that the SN dataset is calibrated and thus do not vary these extra parameters. Our mock dataset includes 2725 SN in the range from $0.01 < z < 3.0$. The existing Pantheon dataset includes SN at $z = 2.3$ [29] so it is not unreasonable that future compilations that build off of the Pantheon compilation could extend even further in redshift. The errors on the distance modulus of each SN ranges from 0.1 magnitudes at $z = 0.01$ to 0.2 magnitudes at $z = 3.0$.

The DESI BAO dataset measures the clustering of galaxies both along the line-of-sight and perpendicular to it and so includes constraints on both the Hubble distance ($D_H(z)$) and the angular diameter distance ($D_M(z)$) individually [1, 4, 6, 7, 10, 28, 32–34]. Because the absolute distance to these galaxies is unknown, the constraints from BAO analyses are expressed as ratios of distances with respect to the sound horizon at drag epoch, r_d :

$$\alpha_{\parallel}(z) = D_H(z)/r_d, \quad \alpha_{\perp}(z) = D_M(z)/r_d. \quad (2)$$

The sound horizon can be thought of as a calibration parameter, and as with the SN, we imagine a case where the calibration is known and thus our mock BAO dataset is just constraints on $D_H(z)$ and $D_M(z)$. DESI is forecasted to measure $D_H(z)$ and $D_M(z)$ in 29 individual redshift bins from $0.05 < z < 3.55$. The precision of each of the measurements can vary from less than 1% to more than 10%.

We generate 100 realizations of the combined datasets for each of the three models in question (see Sec. III) for a total of 300 mock datasets. The seed is fixed for the different models so the residuals are the same. As in, there are only 100 unique realizations of the residuals.

III. MODELS

We consider three distinct models when computing the distribution of the Bayesian evidence and Bayes factors. Specifically we analyze the Λ CDM model, the Transitional Dark Energy (TDE) [13] model, and the Phenomenologically Emergent Dark Energy (PEDE) [20] model. The TDE model is parameterized thusly,

$$w(z) = w_0 + (w_1 - w_0)(-1 - \tanh[(z - z_T)/\Delta]), \quad (3)$$

and we choose $w_0 = -0.8$, $w_1 = -2.0$, $z_T = 1.0$, and $\Delta = 0.2$. The PEDE model has a similar for of the parameterization,

$$w(z) = -\frac{1}{3 \ln 10} (1 + \tanh[\log_{10}(1 + z)]) - 1. \quad (4)$$

The parameters of the TDE model are fixed to put it on a level playing field with PEDE and with Λ CDM. Thus for each of the models, the only free parameters are H_0 and Ω_m . H_0 is allowed to vary between 60 and 80 km sec $^{-1}$ and Ω_m is allowed to vary between 0.0 and 1.0. These models were specifically chosen to be distinguishable given the mock datasets. This is achievable in part because, for the parameters we chose, the TDE model behaves like a quintessent ($w > -1$) dark energy in the region most constrained by the data. On the other hand, the PEDE model exhibits a purely phantom ($w < -1$) behavior. Λ CDM, of course, has a cosmological constant dark energy ($w = -1$). Though both of these models can be thought of as nested extensions to Λ CDM, these types of models are not commonly investigated alternatives to Λ CDM. These models are further interesting since they can encode an evolution in $w(z)$ at different redshifts than $z = 0$, as in the case with the Chevalier-Polarski-Linder [5, 21] (CPL) parameterization $w(z) = w_0 + w_a z/(1 + z)$, which is the most common parameterization of evolving dark energy. So, in summary, we are investigating potential cases where, for example, if TDE is the true model of cosmology, calculating the Bayes factor between Λ CDM and PEDE may favor Λ CDM, but neither are the true model. We show how to use the Bayesian evidence itself to show that both Λ CDM and PEDE are bad fits to the data in such a case.

We also investigate the case where the models in question have different degrees of freedom. Specifically, we look at the cases where we allow the curvature to vary in our models, though the data is still generated from the case where the curvature is fixed to be 0. We call these models where the curvature (Ω_k) is allowed to vary, kTDE, kPEDE, and $k\Lambda$ CDM.

IV. RESULTS

In Fig. 1, we see the distributions of the log evidences for nine different cases (three models were used to generate the data and three models were used for inference).

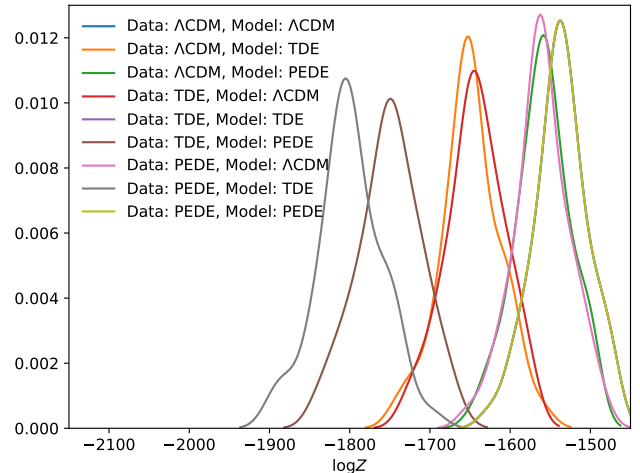


FIG. 1. Distribution of the log evidences for mock datasets generated from the model labelled on the left, inferred using the model labelled on the top. Of particular note is that the distributions for the cases that the model used for the inference is the same as the one used for the data generation are all exactly the same.

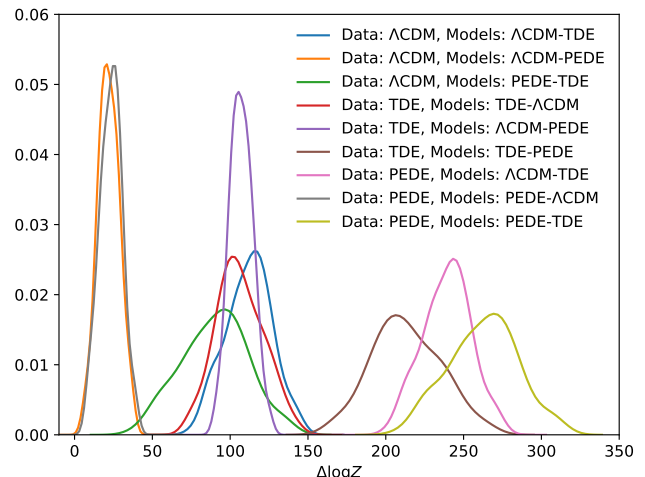


FIG. 2. Distribution of the difference in the log evidence for mock datasets generated from the model labelled on the left, inferred using the models labelled on the top. The labels on the top refer the log evidence of the first model minus the log evidence of the second model.

Of particular note are the cases where the model being used to infer the evidence is the one used to generate the data. The distributions for these cases are exactly the same and lie on top of each other in the figure. This is expected since generating these mock datasets is essentially generating random residuals and these random residuals are the same between the different models. That this distribution of the evidence when the true model is used for inference is the same regardless of model allows us to use it as a robust test of validation, to see if a model is a

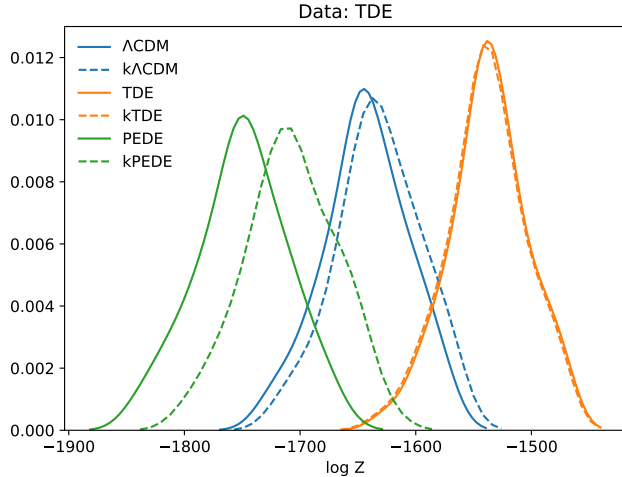


FIG. 3. Distribution of the log evidences for mock realizations from the TDE model inferred using different models when curvature is and is not allowed to vary.

good fit to the data. If the evidence calculated with real data lies outside this distribution, then we can robustly say that model is ruled out, regardless of how well other models perform.

In Fig. 2, we see the distributions of the differences in the log evidences for each of the three pairwise combination of models for each of the three models used to generate the datasets. To explain the figure's labels, the difference is such that $\Delta \log Z = \log Z_L - \log Z_R$ so positive values represent a preference for the model on the left. Basic expectations are borne out by this figure. The model used to generate the data always performs better than a false model. Further, since the TDE model is a quintessential dark energy model in the regime where there is the most data, and since the PEDE model is always phantom, Λ CDM is preferred over the TDE model when the PEDE model is true, and Λ CDM is also preferred over the PEDE model when the TDE model is true. Further, PEDE is closer to Λ CDM and thus it is preferred over TDE when Λ CDM is the true model. That $\Delta \log Z = 0$ is outside the distribution in all these cases indicates that, for this optimistic forecast for DESI BAO data and WFIRST SN data, these classes of dark energy models should be imminently distinguishable. One point that is worth bringing up is that the range of these distributions is noticeably different. This goes to show that using a fixed scale like the Jeffreys or the Kass & Raftery scale cannot serve as one size fits all solutions to the interpretation of Bayes factors. Indeed, for different datasets and different models, one would need to calculate these kinds of distributions to make robust inferences about Bayes factors.

In Fig. 3, we see the distribution of evidences for the specific case of when the data is generated from the TDE model. This figure is useful to make an easy comparison to [17]. This figure also highlights one potential advan-

tage or drawback of Bayesian methods over the distribution of likelihoods from the iterated smoothing method. The Bayesian evidence explicitly uses models and so are more interpretive and thus can say things specifically about model quantities such as curvature. However, because Bayesian methods are more interpretive, they can arrive at wrong conclusions. As is the case in this figure, when the wrong dark energy model is used in the inference Bayesian methods can come to the wrong conclusion about the existence of curvature.

In Fig. 4, we see the distribution of the differences in the log evidences for each of the models when curvature is and is not allowed to vary. This is an example of an additional degree of freedom. In all of these cases, the data was generated from models with no amount of curvature. To explain the figure's labels, the difference is such that $\Delta \log Z = \log Z_{\text{flat}} - \log Z_{\text{curved}}$ and so positive values in the distribution indicate that the flat model is preferred and allowing for this extra degree of freedom is disfavored. Further, focusing on the plots where the models in question are different than the ones used to generate the data, using the wrong dark energy model can, in turn, cause wrong conclusions about whether the Universe is curved. There can either be some amount of confusion between the mismatch in the dark energy models and the curvature (cases where the distribution spans $\Delta \log Z = 0$) or there can be a significant preference for curvature when none was included in the mock datasets, as in the cases where the data was generated with the TDE model but PEDE or Λ CDM were assumed. Further, in the cases where the model used to generate the data is the same as the model used for inference, along with its extension that includes curvature, the distributions of the evidence are roughly equivalent (they each span $\Delta \log Z \in [-1.0, 3]$). In this specific case of using a known model of dark energy and inferring whether curvature is preferred, one could set the criteria for a $> 99\%$ detection of curvature at $\Delta \log Z < -1.0$. Of course, we would not a priori know that we have correctly identified the true model of dark energy. Further, this mapping does not generalize to arbitrary datasets or nested models. For instance, if one were to include different datasets such as weak lensing or the CMB, or were to investigate different models, one would need to recalculate the mapping between Bayes factor and significance.

V. DISCUSSION AND CONCLUSIONS

One advantage of the Bayes factor is that the ratio of two Bayesian evidences cancels out a normalization factor that depends only on the data and not on the models. Here we are using the width of the distribution of $\log Z$ and so the same normalization factor is subtracted off when making the comparison.

The first takeaway from this paper is that the models presented here, and likely any set of DE models, should be distinguishable with future WFIRST and DESI

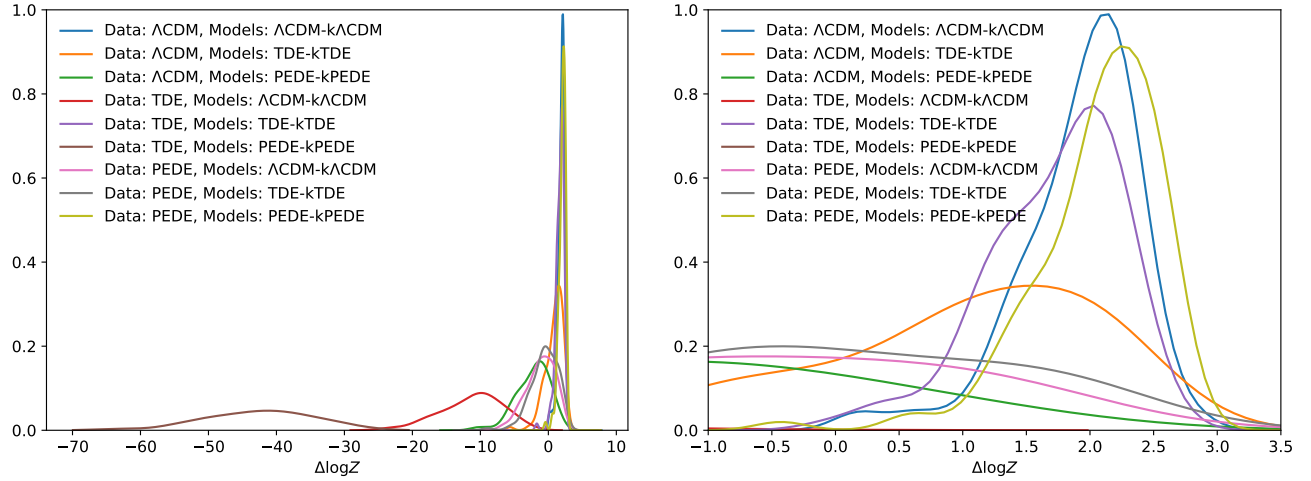


FIG. 4. Distribution of the difference in the log evidence for mock datasets generated from the model labelled on the left, inferred using the models labelled on the top. The difference in the models as labelled on the top, is whether curvature is allowed to vary. The difference in the log evidence is the difference between the flat version of the model minus the version where curvature is free to vary. The right panel is the same as the left but zoomed in on the region $-1.0 < \Delta \log Z < 3.5$

datasets.

The second takeaway is pointing out that the mapping between Bayes factors and p-values depends greatly on the specifics of the dataset, both the size of the covariance matrix and the nature of the datasets (e.g. BAO and SN). This is seen in the fact that the distributions of $\Delta \log Z$ span hundreds of values. Further, the space of the differences in the models will also affect the mapping between a Bayes factor and a p-value. Thus blindly using a fixed scale such as the Jeffreys scale, can be misleading. To accurately asses the significance of a computed Bayes factor, one should perform these kinds of calculations, generate a sample of mock datasets and calculate the Bayes factors in those cases and then see where the Bayes factor for the real dataset lies in that distribution.

Finally, we have shown how to use the evidence itself as a criterion for model validation, to judge if a model is a good fit to the data at all, independently of any other model. Using a distribution of the evidence for mock data generated from a model and inferred using

the same model, one can see if the evidence calculated from the real data lies outside that distribution. Should the evidence computed with real data for a given model fall outside that range, then that model would be invalidated. The distribution of the evidences can be used to calculate the mapping between the Bayesian evidence and a p-value and determine a model-independent criteria to answer the question: “Below what value would the Bayesian evidence have to be to conclude a model is not a good fit to the data?”

ACKNOWLEDGMENTS

We would like to thank Benjamin L’Huillier and Hanwool Koo for useful comments on the draft. This work was supported by the high performance computing cluster Seondeok at the Korea Astronomy and Space Science Institute. A. S. would like to acknowledge the support of the Korea Institute for Advanced Study (KIAS) grant funded by the government of Korea.

-
- [1] Alam S., et al., 2017, MNRAS, 470, 2617
[2] Amanullah R., et al., 2010, ApJ, 716, 712
[3] Béroule M., et al., 2014, A&A, 568, A22
[4] Beutler F., et al., 2017, MNRAS, 464, 3409
[5] Chevallier M., Polarski D., 2001, International Journal of Modern Physics D, 10, 213
[6] DESI Collaboration et al., 2016a, arXiv e-prints, p. arXiv:1611.00036
[7] DESI Collaboration et al., 2016b, arXiv e-prints, p. arXiv:1611.00037
[8] Green J., et al., 2012, arXiv e-prints, p. arXiv:1208.4012
[9] Hicken M., Wood-Vasey W. M., Blondin S., Challis P., Jha S., Kelly P. L., Rest A., Kirshner R. P., 2009, ApJ, 700, 1097
[10] Howlett C., Ross A. J., Samushia L., Percival W. J., Manera M., 2015, MNRAS, 449, 848
[11] Jeffreys H., 1961, Theory of probability. Oxford U.P., Oxford
[12] Kass R. E., Raftery A. E., 1995, Journal of the American Statistical Association, 90, 773
[13] Keeley R. E., Joudaki S., Kaplinghat M., Kirkby D., 2019, J. Cosmology Astropart. Phys., 2019, 035
[14] Keeley R. E., Shafieloo A., Zhao G.-B., Vazquez J. A., Koo H., 2021, AJ, 161, 151

- [15] Koo H., Shafieloo A., Keeley R. E., L'Huillier B., 2020, ApJ, 899, 9
- [16] Koo H., Keeley R. E., Shafieloo A., L'Huillier B., 2021a, arXiv e-prints, p. arXiv:2110.10977
- [17] Koo H., Shafieloo A., Keeley R. E., L'Huillier B., 2021b, J. Cosmology Astropart. Phys., 2021, 034
- [18] Kowalski M., et al., 2008, ApJ, 686, 749
- [19] L'Huillier B., Shafieloo A., Linder E. V., Kim A. G., 2019, MNRAS, 485, 2783
- [20] Li X., Shafieloo A., 2019, ApJ, 883, L3
- [21] Linder E. V., 2003, Phys. Rev. Lett., 90, 091301
- [22] Nesseris S., García-Bellido J., 2013, J. Cosmology Astropart. Phys., 2013, 036
- [23] Perlmutter S., et al., 1999, ApJ, 517, 565
- [24] Planck Collaboration et al., 2020, A&A, 641, A6
- [25] Riess A. G., et al., 1998, AJ, 116, 1009
- [26] Riess A. G., et al., 2007, ApJ, 659, 98
- [27] Riess A. G., Casertano S., Yuan W., Macri L. M., Scolnic D., 2019, ApJ, 876, 85
- [28] Ross A. J., Samushia L., Howlett C., Percival W. J., Burden A., Manera M., 2015, MNRAS, 449, 835
- [29] Scolnic D. M., et al., 2018, ApJ, 859, 101
- [30] Spergel D., et al., 2015, arXiv e-prints, p. arXiv:1503.03757
- [31] Suzuki N., et al., 2012, ApJ, 746, 85
- [32] du Mas des Bourboux H., et al., 2017, A&A, 608, A130
- [33] du Mas des Bourboux H., et al., 2020, arXiv e-prints, p. arXiv:2007.08995
- [34] eBOSS Collaboration et al., 2020, arXiv e-prints, p. arXiv:2007.08991